



CASE REPORT

Managing severe curvature of radix entomolaris: three-dimensional analysis with cone beam computed tomography

F. Abella, M. Mercadé, F. Duran-Sindreu & M. Roig

Department of Endodontics, Universitat Internacional de Catalunya, Sant Cugat del Vallès, Barcelona, Spain

Abstract

Abella F, Mercadé M, Duran-Sindreu F, Roig M. Managing severe curvature of radix entomolaris: three-dimensional analysis with cone beam computed tomography. *International Endodontic Journal*, **44**, 876–885, 2011.

Aim To present a case of a mandibular first molar with an additional distolingual root [radix entomolaris (RE)] and to discuss the use of cone beam computed tomography (CBCT) for its identification and management during root canal treatment.

Summary A 52-year-old Caucasian woman was referred for root canal treatment of the right mandibular first molar (tooth 46). After clinical and radiographic examination, a symptomatic irreversible pulpitis was diagnosed. Three periapical radiographs with different horizontal angulations revealed the presence of an additional distolingual root. This extra root, termed RE, has an incidence of <5% in the Caucasian population. A CBCT examination was also taken, which revealed a severe root canal curvature, especially in the middle third, of this supernumerary root. CBCT provided more accurate information in terms of RE inclination and root canal curvature before commencing root canal treatment. The conventional access opening was modified into a more trapezoidal cavity, and five root canals were found. All canals were instrumented with new nickel–titanium (NiTi) files to reduce the risk of fractured instruments. After preparation, the root canals were filled using thermoplastified techniques. The 1-year follow-up periapical radiographs and CBCT images revealed a continuous periodontal space with no signs of apical periodontitis.

Key learning points

- Cone beam computed tomography imaging is useful in identifying the root canal system and the surrounding structures.
- An accurate detection of supernumerary roots, such as RE, can avoid complications during and after root canal treatment.

Correspondence: Miguel Roig, Dentistry Faculty, Universitat Internacional de Catalunya, C/Josep Trueta s/n. 08195, Sant Cugat del Vallès, Barcelona, Spain (Tel.: + 34 504 2000; fax: +34 504 2031; e-mail: mroig@csc.uic.es).

- The analysis of root canal curvature is important because instrument fracture has been linked to angle and radius of curvature.
- The use of new instruments can reduce the incidence of instrument fracture.

Keywords: anatomical variations, cone beam computed tomography, radix entomolaris, root canal curvature.

Received 10 February 2011; accepted 9 May 2011

Introduction

A number of teeth do not respond to root canal treatment because of persistent infection caused by a missing canal and to failure to remove all the pulp tissue and microorganisms from the root canal system (Byström *et al.* 1987, Sjögren *et al.* 1997). In short, an awareness and understanding of root canal anatomy will help to improve the outcome of treatment.

Most mandibular first molars have two roots located mesially and distally and three root canals (Barker *et al.* 1974, Vertucci 1984), but variations in the number of roots and in canal morphology are not uncommon (Skidmore & Bjørndal 1971). The major variant is the occurrence of an additional third root, a supernumerary root typically found lingually. This was first reported by Carabelli (1884) and was termed radix entomolaris (RE) (Bolk 1915). This extra root is typically smaller than the distobuccal root and is usually curved. The relevant literature revealed an incidence of <5% in Caucasian, African, Eurasian and Indian populations, whereas in those with Mongoloid traits, such as Chinese, Eskimo and Native American populations, the RE occurs with a frequency of 5% and even up to 40% (Gulabivala *et al.* 2001, De Moor *et al.* 2004, Tu *et al.* 2007, Chen *et al.* 2009, Huang *et al.* 2010).

The recent introduction of cone beam computed tomography (CBCT) scans provides three-dimensional information and a number of useful applications in endodontics (Cotton *et al.* 2007). One of CBCT's major advantages over computed tomography (CT) scanners is the reduction in radiation exposure (Cotton *et al.* 2007, Patel *et al.* 2007, Scarfe & Farman 2008). CBCT imaging is useful in identifying the root canal system (Matherne *et al.* 2008) and can even determine the exact position of the distolingual root of the permanent mandibular first molars (Tu *et al.* 2009).

The present report describes the clinical detection of a RE by using CBCT imaging and root canal treatment in a right mandibular first molar with five canals, three of which are located in two distal roots.

Report

A 52-year-old Caucasian woman was referred by her general dental practitioner for root canal treatment of the right mandibular first molar (tooth 46). The medical history was non-contributory. Clinical examination showed an occlusal restoration (Fig. 1a). The patient complained of spontaneous toothache. The tooth was both cold and heat sensitive. Radiographic examination showed no signs of apical periodontitis (Fig. 1b–d). The clinical diagnosis of symptomatic irreversible pulpitis was made, and root canal treatment was scheduled. Three radiographs with different horizontal angulations (Fig. 1b–d) were taken with Kodak RVG 6100 digital radiography system (Carestream Health, Rochester, NY, USA). Interpretation of off-angle radiographs revealed the presence of an additional lingual root.

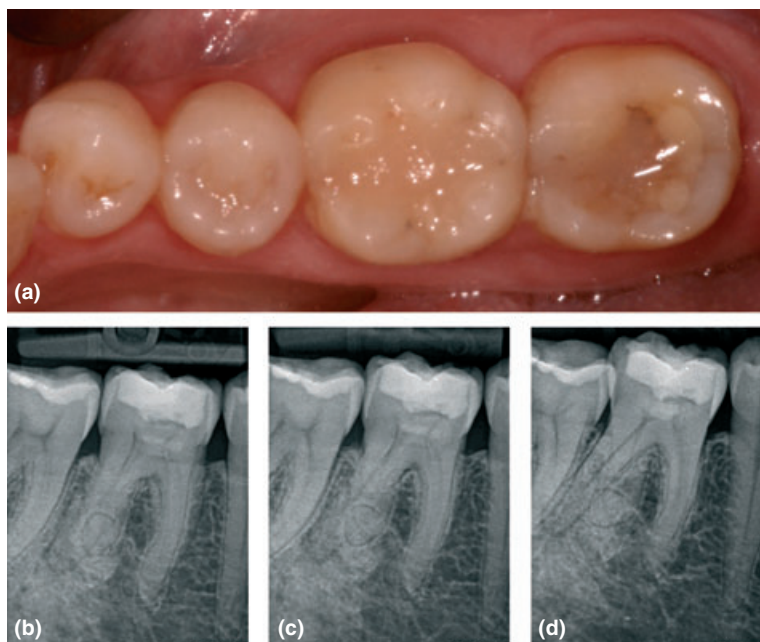


Figure 1 (a) Tooth 46 with coronal restoration. Preoperative periapical radiographs (parallax technique) of tooth 46 with different horizontal angulations. (b) ortho-, (c) mesioradial and (d) distoradial.

A small volume CBCT was taken using Kodak 9000 3D (Carestream Health) to reveal the exact location and direction of this supernumerary root. The morphology of the tooth was obtained in coronal, axial and sagittal sections (Figs 2,3 and 4). The sagittal images showed a pronounced curve in the middle part of the root canal of the RE (Fig. 2). According to the classification of De Moor *et al.* (2004), this RE corresponds to type III. This type suggests an initial curve in the coronal third of the root canal and a second curve beginning in the middle and continuing to the apical third.

After anaesthesia and isolation with rubber dam (Hygenic Dental Dam, Coltène Whaledent, Langenau, Germany), an endodontic access cavity was prepared. When the floor of the pulp chamber was reached, four canal orifices were initially identified (Fig. 5a). After extending the access cavity towards the lingual with an ultrasonic diamond-coated tip (ET 18D; Satelec Acteon Group, Merignac, France), a third distal canal was found with a size 10 K-file (Dentsply Maillefer, Ballaigues, Switzerland) (Fig. 5b,c). Figure 5(d) shows the final access cavity form.

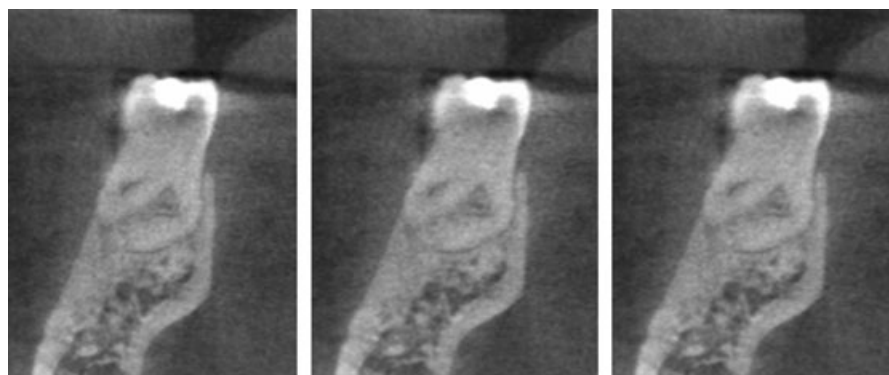


Figure 2 Sagittal views reveal the presence of radix entomolaris in tooth 46.

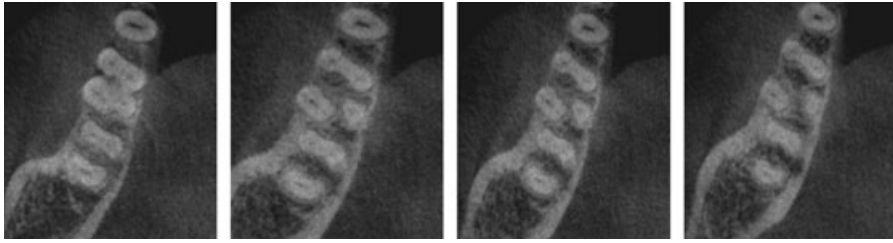


Figure 3 Axial views allow the relationship between the supernumerary root and the other roots to be assessed.

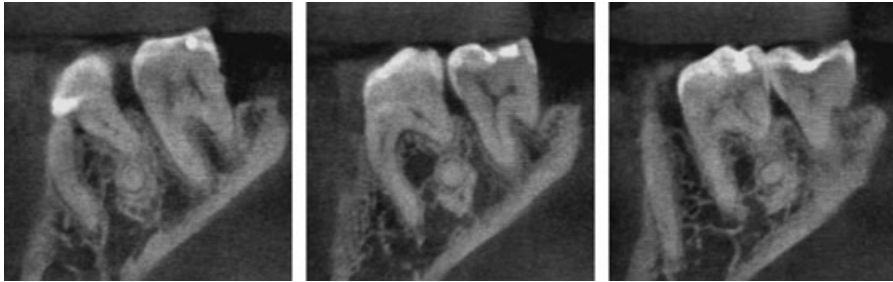


Figure 4 Different coronal views of tooth 46.



Figure 5 (a) Occlusal view of the pulp chamber with four canal orifices. (b) Enlargement of the access cavity. (c) Location of a third distal canal orifice. (d) Final access cavity.

The root lengths were estimated using an apex locator (Root ZX; Morita, Tokyo, Japan) and then confirmed with a periapical radiograph (Fig. 6a). Coronal flaring of the root canals was carried out using S1 and SX ProTaper rotary instruments (Dentsply Maillefer,

Ballaigues, Switzerland). All canals were instrumented with a size 10 and 15 K-file (Dentsply Maillefer, Ballaigues, Switzerland) to obtain a manual glide path. Instrumentation was completed using Mtwo (VDW GmbH, Munich, Germany) nickel–titanium (NiTi) rotary instruments with X-Smart endodontic motor (Dentsply Maillefer, Ballaigues, Switzerland). The instrumentation sequence for the RE was size 10, 0.04; 15, 0.05; and 20, 0.06, and for the other roots canals, 10, 0.04; 15, 0.05; 20, 0.06; 25, 0.06; 30, 0.05 and 35, 0.04.

During instrumentation, the root canals were flushed with copious amounts of 4.2% sodium hypochlorite (NaOCl) solution using a plastic syringe with a closed-end needle (Hawe Max-I-probe; Kerr-Hawe, Bioggio, Switzerland). After root canal preparation, a final irrigation was performed alternating 17% ethylenediaminetetraacetic acid and 4.2% NaOCl solution. The last NaOCl solution was activated with a size 15 K-file (Satelec Acteon Group) under passive ultrasonic activation for 1 min (Fig. 6b). The root canals were then washed with sterile saline and dried with sterile paper points. After preparation, gutta-percha cones (Autofit; Analytic, Glendora, CA, USA) and a size 20 Thermafil verifier (Dentsply Maillefer, Ballaigues, Switzerland) were used to reconfirm working lengths (Fig. 6c).

The additional lingual root canal was filled with a size 20 Thermafil obturator (Dentsply Maillefer, Ballaigues, Switzerland) and AH-Plus cement (Dentsply DeTrey GmbH, Konstanz, Germany). The other root canals were filled using the System B heat source (EIE/Analytic Technology, Richmond, WA, USA) (Fig. 7a,b). The access cavity was restored with a resin composite flow (Tetric Flow; Ivoclar Vivadent AG, Schaan Furstentum, Liechtenstein) to ensure an adequate seal between appointments, and a temporary restorative material (Cavit; 3M ESPE AG, Seefeld, Germany) (Fig. 7c).

The final restoration was an indirect composite resin (in:joy; DeguDent GmbH, Hanau-Wolfgang, Germany). The 1-year follow-up periapical radiographs showed a continuous periodontal space with no signs of apical periodontitis (Fig. 8).

Thereafter, another small-volume CBCT was taken (Kodak 9000 3D; Carestream Health) to determine the success of treatment. A healthy periapex was confirmed according to the axial (Fig. 9a,b), sagittal (Fig. 9c,d) and coronal slices (Fig. 10a,b) and the three-dimensional reconstruction (Fig. 10c).

Discussion

The RE is located distolingually, with its coronal third completely or partially fixed to the distal root. In general, the RE is smaller than the distobuccal and mesial roots and can be separated from, or partially fused with, the other roots. According to the classification of De Moor *et al.* (2004), the RE could be classified into three groups on the basis of the root/

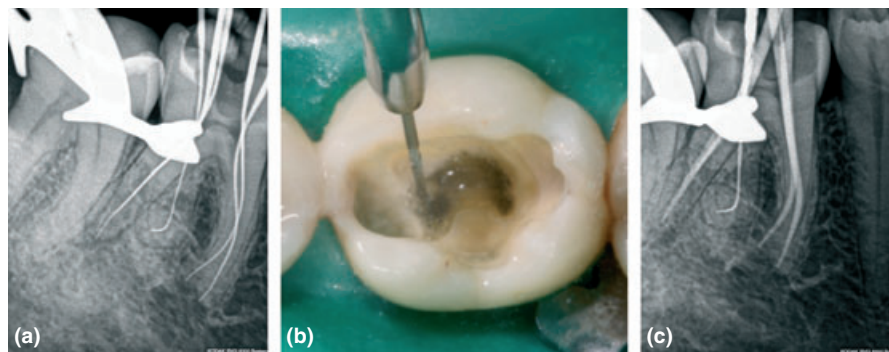


Figure 6 (a) Length determination radiograph. (b) Passive ultrasonic activation. (c) Gutta-percha cones and 20 Thermafil verifier (Dentsply Maillefer) before root canal filling.

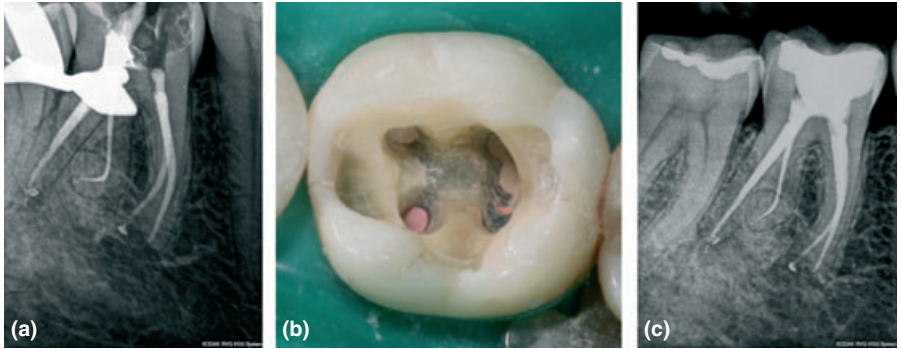


Figure 7 (a) Radiographic control following filling of the five root canals. (b) Clinical image of the access cavity after root canal filling. (c) Postoperative radiograph.

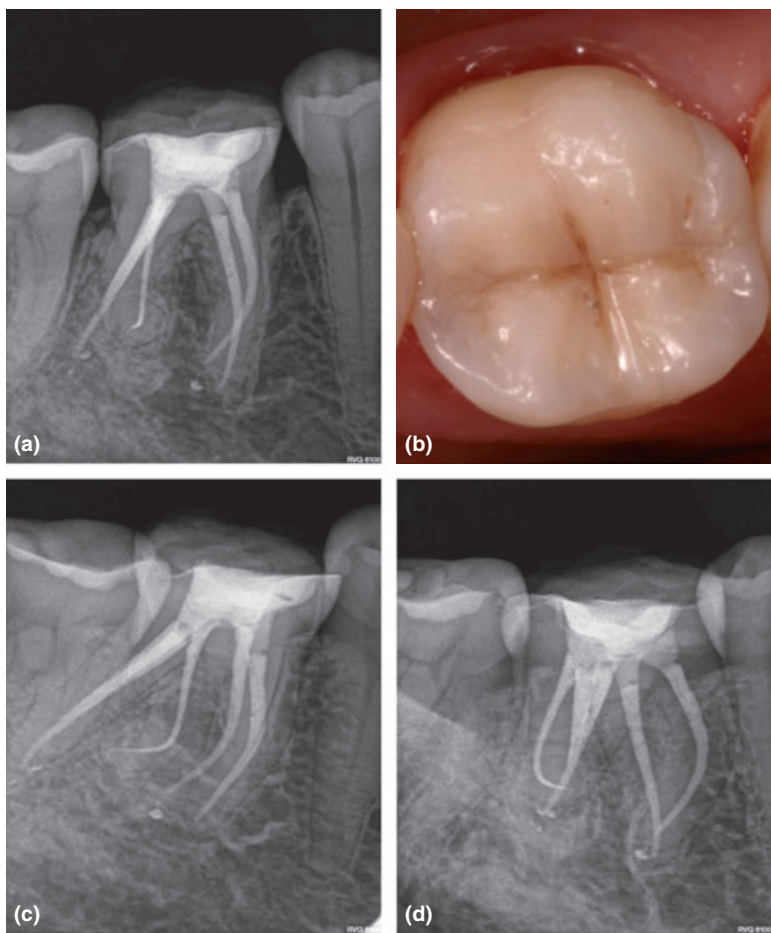


Figure 8 (a) Radiograph 1-year postoperatively. (b) Occlusal view of tooth 46 restoration. (c) A mesioradial and (d) distoradial postoperative radiographs.

root canal curve. Type I refers to a straight root canal, type II refers to an initially curved entrance that continues as a straight canal and type III refers to an initial curve in the coronal third of the root canal and a second curve beginning in the middle and continuing

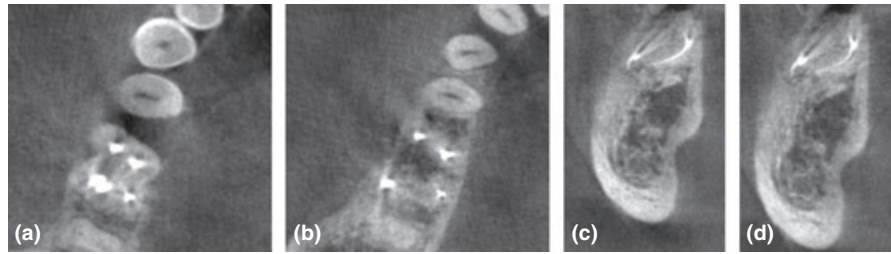


Figure 9 (a, b) Cone beam computed tomography axial and (c, d) sagittal slices showed normal periapical area of tooth 46.

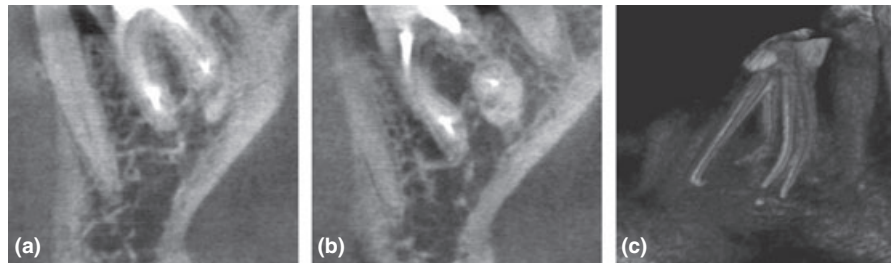


Figure 10 (a, b) Coronal cone beam computed tomography views. (c) Three-dimensional reconstruction of tooth 46 after root canal filling.

to the apical third. An accurate detection of these supernumerary roots can avoid complications or a 'missed canal' during root canal treatment. Because the (separate) RE is mostly situated in the same bucco-lingual plane as the distobuccal root, a superimposition of both roots can appear on the preoperative radiograph, resulting in an inaccurate detection. Conventional images compress three-dimensional anatomy into a two-dimensional image or shadowgraph. Important features of the tooth are visualized in the mesiodistal plane only. However, similar features shown in the bucco-lingual plane (i.e. the third dimension) may not be fully appreciated. In an attempt to overcome the limitations of plain radiography, additional exposures with changes in horizontal tubehead angulation (parallax principle) may be considered (Fava & Dummer 1997). To reveal the RE, a second radiograph should be taken from a more distal or mesial angle (30°). However, it should be noted that multiple intra-oral radiographs do not guarantee the identification of all relevant anatomies. Three-dimensional imaging overcomes this major limitation by allowing the visualization of the third dimension whilst at the same time eliminating superimpositions (Cohenca *et al.* 2007b). However, at present, the images produced with CBCT technology lack the resolution of conventional radiographs. To ascertain the exact location and anatomy of the RE, a CBCT scanner was used to obtain a better analysis. CBCT is a technique that produces three-dimensional digital imaging at reduced cost and less radiation for the patient than traditional CT scans (Cohenca *et al.* 2007b). If an RE is diagnosed before root canal treatment, one knows what to expect or where to look once the pulp chamber has been opened.

The location of the orifice of the root canal of an RE has implications for the access cavity. The orifice of the RE is located disto- to mesiolingually from the main canal or canals in the distal root. Hence, the conventional access opening was modified into a more trapezoidal cavity to locate the orifice of the distolingually located RE. A dark line on the pulp chamber could indicate the precise location of the RE canal orifice. If the RE orifice is not clearly visible after removal of the pulp chamber roof, a more meticulous

inspection in the distolingual region is necessary; visual aids with loupes or surgical operating microscope could be useful (Yoshioka *et al.* 2002). RE canal orifice could be occluded by secondary or calcified dentine. With every access preparation in a calcified root, there is a risk of perforating the tooth. When searching for hidden canals, one should remember that secondary dentine is generally whitish or opaque, whereas the floor chamber is darker and grey in appearance. Therefore, the visual access and superior control that ultrasonic cutting tips provide during access procedures make them a convenient tool in such cases (Plotino *et al.* 2007).

The case presented was classified as type III RE, because a severe canal curvature (great angle and small radius of curvature), especially in the middle and apical third, was observed in the CBCT. In this case, NiTi rotary instruments were used, as several studies have shown that these instruments are able to maintain original canal curvature even in severely curved canals, to produce a well-tapered root canal shape sufficient for filling and to complete preparation in an acceptable time (Sonntag *et al.* 2003, Moore *et al.* 2009, Uroz-Torres *et al.* 2009). However, the advent of rotary NiTi files has been accompanied by an unfortunate increase in the occurrence of broken instruments (Ruddle 2004). For this reason, after relocation and enlargement of the orifice of the RE, a manual glide path should be performed, because this procedure drastically reduces torsional stress as the canal width becomes at least equal to the diameter of the tip of the instrument used (Berutti *et al.* 2004). Knowing and analysing root canal curvature is important because instrument fracture has been linked to angle and radius of curvature. The cyclic fatigue of an instrument may be related to the degree of flexure it undergoes when placed in a curved root canal. The more pronounced the curvature of a canal, the greater the cyclical fatigue of the instrument and thus the lower its life expectancy. Instrument separation significantly increased as the radius of curvature decreased (Pruett *et al.* 1997, Zelada *et al.* 2002, Patiño *et al.* 2005, Grande *et al.* 2006, Inan *et al.* 2007). Different authors observed that fatigue life of NiTi rotary instruments was significantly influenced by the radius of curvature (Pruett *et al.* 1997, Grande *et al.* 2006). Zelada *et al.* (2002) reported that radius of curvature was the most important factor in instrument fracture, and in canals with small radius of curvature, the risk of instrument fracture was greater. It has been observed that a reduction in the angle of curvature produced a significant decrease in the incidence of instrument fracture. In this case, new instruments were used because instrument fracture significantly increased with the number of uses (Patiño *et al.* 2005, Vieira *et al.* 2008).

A CBCT was also taken 1-year postoperatively, because it has been reported that CBCT scans detect periapical lesions in many cases in which periapical radiolucency was absent in the periapical radiograph (Lofthag-Hansen *et al.* 2007, Jorge *et al.* 2008). In fact, recent studies corroborate the use of CBCT as the standard radiographic control to guarantee the successful outcome of root canal treatment (Estrela *et al.* 2008a, Vandenberghe *et al.* 2008, Paula-Silva *et al.* 2009a, Wu *et al.* 2009). In addition, one of the major advantages of limited CBCT is the significantly lower effective radiation dose to which patients are exposed (Cohenca *et al.* 2007b, Patel 2009).

Conclusions

Clinicians should be aware of the unusual anatomical features and variations in the mandibular first molars in Caucasians. Root canal treatment in teeth with extra roots can be challenging, but the inability to find root canals may cause failures. CBCT images can result in a better understanding of root canal anatomy, which enables the clinician to evaluate the root canal system and to clean, shape and fill it more efficiently.

Disclaimer

Whilst this article has been subjected to Editorial review, the opinions expressed, unless specifically indicated, are those of the author. The views expressed do not necessarily represent best practice, or the views of the IEJ Editorial Board, or of its affiliated Specialist Societies.

References

- Barker BC, Parsons KC, Mills PR, Williams GL (1974) Anatomy of root canals. III. Permanent mandibular molars. *Australian Dental Journal* **19**, 408–13.
- Berutti E, Negro AR, Lendini M, Pasqualini D (2004) Influence of manual preflaring and torque on the failure rate of ProTaper rotary instruments. *Journal of Endodontics* **30**, 228–30.
- Bolk L (1915) Bermerkungen über Wurzelvariationen am menschlichen unteren Molaren. *Zeitung für Morphologie und Anthropologie* **17**, 605–10.
- Byström A, Happonen R-P, Sjögren U, Sundqvist G (1987) Healing of periapical lesions of pulpless teeth after endodontic treatment with controlled asepsis. *Endodontics & Dental Traumatology* **3**, 58–63.
- Carabelli G (1884) *Systematisches Handbuch der Zahnheilkunde*, 2nd edn. Vienna, Austria: Braumüller and Seidel, pp. 114.
- Chen G, Yao H, Tong C (2009) Investigation of the root canal configuration of mandibular first molars in a Taiwan Chinese population. *International Endodontic Journal* **42**, 1044–9.
- Cohenca N, Simon JH, Marthur A, Malfaz JM (2007b) Clinical indications for digital imaging in dento-alveolar trauma. Part 2: root resorption. *Dental Traumatology* **23**, 105–13.
- Cotton TP, Geisler TM, Holden DT, Scwartz SA, Schindler WG (2007) Endodontic applications of cone-beam volumetric tomography. *Journal of Endodontics* **33**, 1121–32.
- De Moor RJ, Deroose CA, Calberson FL (2004) The radix entomolaris in mandibular first molars: an endodontic challenge. *International Endodontic Journal* **37**, 789–99.
- Estrela C, Bueno MR, Leles CR, Azevedo B, Azevedo B, Azevedo JR (2008a) Accuracy of cone beam computed tomography and panoramic and periapical radiography for detection of apical periodontitis. *Journal of Endodontics* **34**, 273–9.
- Fava LR, Dummer PM (1997) Periapical radiographic techniques during endodontic diagnosis and treatment. *International Endodontic Journal* **30**, 250–61.
- Grande NM, Plotino G, Pecci R, Bedini R, Malagnino VA, Somma F (2006) Cyclic fatigue resistance and three-dimensional analysis of instruments from two nickel-titanium rotary systems. *International Endodontic Journal* **39**, 755–63.
- Gulabivala K, Aung TH, Alavi A, Ng Y-L (2001) Root and canal morphology of Burmese mandibular molars. *International Endodontic Journal* **34**, 359–70.
- Huang RY, Cheng WC, Chen CJ *et al.* (2010) Three-dimensional analysis of the root morphology of mandibular first molars with distolingual roots. *International Endodontic Journal* **43**, 478–84.
- Inan U, Aydin C, Uzun O, Topuz O, Alacam T (2007) Evaluation of the surface characteristics of used and new ProTaper instruments: an atomic force microscopy study. *Journal of Endodontics* **33**, 1334–7.
- Jorge EG, Tanomaru-Filho M, Gonçalves M, Tanomaru JMG (2008) Detection of periapical lesion development by conventional radiography or computed tomography. *Oral Surgery, Oral Medicine, Oral Pathology, Oral Radiology, and Endodontics* **106**, e56–61.
- Lofthag-Hansen S, Huuonen S, Gröndahl K, Gröndahl HG (2007) Limited cone beam CT and intraoral radiography for the diagnosis of periapical pathology. *Oral Surgery, Oral Medicine, Oral Pathology, Oral Radiology, and Endodontics* **103**, 114–9.
- Matherne RP, Angelopoulos C, Kulid JC, Tira D (2008) Use of cone-beam computed tomography to identify root canal systems in vitro. *Journal of Endodontics* **34**, 87–9.
- Moore J, Fitz-Walter P, Parashos P (2009) A micro-computed tomographic evaluation of apical root canal preparation using three instrumentation techniques. *International Endodontic Journal* **42**, 1057–64.

- Patel S (2009) New dimensions in endodontic imaging: Part 2. Cone beam computed tomography. *Journal of Endodontics* **42**, 463–75.
- Patel S, Dawood A, Whites E, Pitt Ford T (2007) The potential applications of cone beam computed tomography in the management of endodontic problems. *International Endodontic Journal* **40**, 818–30.
- Patiño PV, Biedma BM, Liébana CR, Cantatore G, Bahillo JG (2005) The influence of a manual glide path on the separation rate of NiTi rotary instruments. *Journal of Endodontics* **31**, 114–6.
- Paula-Silva FWG, Hassan B, da Silva LAB, Leonardo MR, Wu M-K (2009a) Outcome of root canal treatment in dogs determined by periapical radiography and cone beam computed tomography. *Journal of Endodontics* **35**, 723–6.
- Plotino G, Pameijer CH, Grande NM, Somma F (2007) Ultrasonics in endodontics: a review of the literature. *Journal of Endodontics* **33**, 81–95.
- Pruett JP, Clement DJ, Carnes DL Jr (1997) Cyclic fatigue testing of nickel-titanium endodontic instruments. *Journal of Endodontics* **23**, 77–85.
- Ruddle CJ (2004) Nonsurgical retreatment. *Journal of Endodontics* **30**, 827–45.
- Scarfe WC, Farman AG (2008) What is cone-beam CT and how does it work? *Dental Clinics of North America* **52**, 707–30.
- Sjögren U, Figdor D, Persson S, Sundqvist G (1997) Influence of infection at the time of root filling on the outcome of endodontic treatment of teeth with apical periodontitis. *International Endodontic Journal* **30**, 297–306.
- Skidmore AE, Bjorndal AM (1971) Root canal morphology of the human mandibular first molar. *Oral Surgery, Oral Medicine, and Oral Pathology* **32**, 778–84.
- Sonntag D, Guntermann A, Kim SK, Stachniss V (2003) Root canal shaping with manual stainless steel files and rotary Ni-Ti files performed by students. *International Endodontic Journal* **36**, 246–55.
- Tu MG, Tsai CC, Jou MJ *et al.* (2007) Prevalence of three-rooted mandibular first molars among Taiwanese individuals. *Journal of Endodontics* **33**, 1163–6.
- Tu MG, Huang HL, Hsue SS *et al.* (2009) Detection of permanent three-rooted mandibular first molars by cone-beam computed tomography imaging in Taiwanese individuals. *Journal of Endodontics* **35**, 503–7.
- Uroz-Torres D, González-Rodríguez MP, Ferrer-Luque CM (2009) Effectiveness of a manual glide path on the preparation of curved root canals by using Mtwo rotary instruments. *Journal of Endodontics* **35**, 699–702.
- Vandenbergh B, Jacobs R, Yang J (2008) Detection of periapical bone loss using digital intraoral and cone beam computed tomography images: an in vitro assessment of bony and/or infrabony defects. *Dento Maxillo Facial Radiology* **37**, 252–60.
- Vertucci FJ (1984) Root canal anatomy of the human permanent teeth. *Oral Surgery, Oral Medicine, and Oral Pathology* **58**, 589–99.
- Vieira EP, França EC, Martins RC, Buono VT, Bahia MG (2008) Influence of multiple clinical use on fatigue resistance of ProTaper rotary nickel-titanium instruments. *International Endodontic Journal* **41**, 163–72.
- Wu M-K, Shemesh H, Wesselink PR (2009) Limitations of previously published systematic reviews evaluating the outcome of endodontic treatment. *International Endodontic Journal* **42**, 656–66.
- Yoshioka T, Kobayashi C, Suda H (2002) Detection rate of root canal orifices with a microscope. *Journal of Endodontics* **28**, 452–3.
- Zelada G, Varela P, Martín B, Bahillo JG, Magán F, Ahn S (2002) The effect of rotational speed and the curvature of root canals on the breakage of rotary endodontic instruments. *Journal of Endodontics* **28**, 540–2.

This document is a scanned copy of a printed document. No warranty is given about the accuracy of the copy. Users should refer to the original published version of the material.